



Contents lists available at ScienceDirect

Saudi Pharmaceutical Journal

journal homepage: [www.sciencedirect.com](http://www.sciencedirect.com)

Original article

# Influence of nanofiber alignment on the release of a water-soluble drug from cellulose acetate nanofibers

Prasopchai Patrojanasophon, Siripran Tidjarat, Praneet Opanasopit, Tanasait Ngawhirunpat, Theerasak Rojanarata\*

Pharmaceutical Development of Green Innovations Group (PDGIG), Faculty of Pharmacy, Silpakorn University, Nakhon Pathom 73000, Thailand

## ARTICLE INFO

### Article history:

Received 20 April 2020

Accepted 11 August 2020

Available online 17 August 2020

### Keywords:

Drug release  
Nanofiber alignment  
Cellulose acetate  
Nanofibers  
Water-soluble drug

## ABSTRACT

Cellulose acetate nanofibers with different degrees of alignment (randomly aligned (RA), partially aligned (PA), and highly aligned (HA)) were produced using an electrospinning technique. The different degrees of alignment were obtained by adjusting the rotation speed of the collector. Alpha-arbutin (3% w/w) employed as a model water-soluble compound was incorporated into the nanofibers during the fabrication process. The drug release characteristics were investigated using the nanofiber mats with the same size and weight. The prepared nanofibers with different degrees of alignment showed similar physical characteristics, including the fiber diameter, drug loading efficiency and capacity, and molecular form of the drug in the fibers. Interestingly, alpha-arbutin was released from HA nanofibers at a significantly faster rate than the PA and RA nanofibers. Eighty percent of the drug was released into the medium in 1.7, 4.2, and 9.4 min for HA, PA, and RA nanofibers, respectively. The orientation of nanofibers played a crucial role in governing the drug release, probably by creating network meshes with different degrees of entanglement, affecting the diffusion of drug to the external medium. Consequently, this approach can be used as a simple means of achieving immediate-release or fast-acting characteristics of cellulose-based formulations containing a water-soluble drug.

© 2020 The Author(s). Published by Elsevier B.V. on behalf of King Saud University. This is an open access article under the CC BY-NC-ND license (<http://creativecommons.org/licenses/by-nc-nd/4.0/>).

## 1. Introduction

Recently, many scientific researchers have developed novel dosage forms with a fast-acting effect to obtain quick action of drugs and enhanced bioavailability (Perissutti et al., 2003; Tonglairoum et al., 2014). Due to the advance in technology, nano-based materials have acquired lots of attention. Nanofiber-based materials are becoming more popular due to their marvelous characteristics such as high flexibility, low density, huge porosity, high specific surface areas and tiny pore sizes (Hu et al., 2014). Electrospinning is an uncomplicated and popular method used to fabricate nanosized or microsized fibers employing an electrostatic field to stretch the polymer droplet to form nanofibers (Thenmozhi et al., 2017; Vong et al., 2018). The process of

electrospinning has been widely applied in several fields such as tissue engineering, drug delivery systems, wound dressing, filtration, etc. (Haider et al., 2018; Teo and Ramakrishna, 2006; Tonglairoum et al., 2015). Electrospun nanofibers exhibit excellent features, making them appealing as drug carriers. The high surface area of nanofibers surmounts the limitation of conventional dosage form. Fabrication of ultrafine electrospun nanofiber is a promising way to develop oral fast-dissolving dosage forms. It not only improves the solubility of the drug, but also provides rapid drug release (Pillay et al., 2013; Tonglairoum et al., 2014).

Facial masks are popular beauty treatments used to improve skin quality. Conventional beauty face masks available in the market are cotton masks that are pre-moistened with skin nutrients (Fathi-Azarbayjani et al., 2010). Skin whitening face masks are also commercially available for cosmetic purposes in order to obtain a lighter skin appearance, and they are popular in Asian countries. Alpha-arbutin is one of the most commonly used skin-brightening compound. It is a highly water soluble plant-derived substance, which inhibits tyrosinase enzyme and melanosome maturation (Maeda et al., 1996; Sarkar et al., 2013). In addition, alpha-arbutin has found to be less toxic than hydroquinone (Sarkar et al., 2013). A nanofiber-based anti-wrinkle face mask

\* Corresponding author.

E-mail address: [rojanarata\\_t@su.ac.th](mailto:rojanarata_t@su.ac.th) (T. Rojanarata).  
Peer review under responsibility of King Saud University.



Production and hosting by Elsevier

has been previously developed by Fathi-Azarbayjani et al. The masks could provide fast release of the active compounds and exhibit high skin penetration due to the high surface area of nanofibers (Fathi-Azarbayjani et al., 2010).

Cellulose acetate (CA) is a polymer of choice in producing a number of materials. Electrospun CA fibers demonstrates remarkable properties, including biocompatibility, water insolubility, good mechanical properties, low toxicity, excellent hydrolytic stability, low cost, and excellent chemical resistance (Khoshnevisan et al., 2018; Konwarh et al., 2013). It, therefore, have been employed in various applications; for example, tissue engineering, sensors, nutraceutical and drug delivery, etc. (Konwarh et al., 2013).

Fast release of active compound from a delivery system seems to be beneficial in cosmetic and pharmaceutical fields as it could provide fast-acting effect and high customer satisfaction. Many factors influencing the release of drug from nanofibers, including the types of polymer used to form nanofibers, the nanofiber diameter, porosity, geometry, and morphology, have been reported (Akhgari et al., 2017; Chou and Woodrow, 2017). However, the studies which focused on the the effect of nanofiber alignment on drug release from nanofibers are limited. Eslamian et al compared the release of a hydrophobic drug, dexamethasone, from randomly oriented and aligned hydrophobic poly(lactide-co-glycolide) nanofibers. They found an initial burst release of the drug in the first 24 h followed by a sustained release for the next 24 days. The aligned fibers had less burst release and more sustained release compared to the random ones (Eslamian et al., 2019). Meng et al evaluated the release of poorly water-soluble fenbufen from PLGA, PLGA/gelatin, and PLGA/chitosan nanofibers. They revealed that the release rate of the drug from the aligned nanofibers was less than that from the randomly oriented nanofibers as the aligned nanofibers had increased density and decreased pore size of scaffolds compared with the randomly oriented ones (Meng et al., 2011a, 2011b). Nevertheless, the study investigating the effect of fiber alignment on the release of hydrophilic drug from hydrophobic nanofibers is still lacking.

Herein, the influence of nanofiber alignment on the release of a hydrophilic drug from hydrophobic cellulose acetate nanofibers had been investigated. Cellulose acetate nanofibers were generated by an electrospinning technique. The orientation of the fibers was varied by adjusting the collector rotation speed to obtain randomly aligned (RA), partially aligned (PA), and highly aligned (HA) nanofibers. Alpha-arbutin was selected as a model compound to be incorporated into CA nanofibers, and the release characteristics of the drug from the nanofibers were investigated.

## 2. Material and methods

### 2.1. Materials

Cellulose acetate (CA; Mw = 30 kDa; the degree of acetylation ≈ 2.4) and alpha-arbutin were obtained from Sigma Aldrich® (St. Louis, MO, USA). All the solvents used were of analytical grade and were used as received unless otherwise stated.

### 2.2. Electrospinning of alpha-arbutin-loaded CA nanofibers

Alpha-arbutin-loaded CA nanofibers with different degrees of alignment were fabricated by electrospinning process. Briefly, CA (17 %w/v) and alpha-arbutin (3 %wt to polymer) were dissolved in a solvent mixture of acetone and *N,N*-dimethylacetamide (2:1 v/v), and the mixture was stirred overnight. Afterward, the mixture was filled in a 5-mL syringe connected to a stainless steel needle

(20G, an inner diameter of 0.9 mm) and linked to a high voltage power supply (17.5 kV). The feeding rate was controlled at 0.4 mL/h using a syringe pump, and the tip-to-collector distance was fixed at 15 cm. The nanofibers were collected on an aluminium foil covering the grounded collector (diameter ≈ 19 cm). The rotating speed of the collector was varied (350, 2000 and 6000 rpm) to produce the nanofibers with different degrees of uniaxial alignment. To obtain the nanofibers with equivalent weight per area, the electrospinning was continued for 5, 8, and 12 h for the rotation speed of 350, 2000 and 6000 rpm, respectively. The electrospinning setup is displayed in Fig. 1.

### 2.3. Characterization of alpha-arbutin-loaded CA nanofibers

#### 2.3.1. Morphological characterizations

The morphologies, fiber orientation, diameters and thickness of the CA electrospun nanofibers were assessed using a scanning electron microscope (SEM, Camscan Mx2000, England). Each fiber was cut into a small piece and then coated with a thin layer of gold prior to the SEM observation. The fiber diameter and the thickness of the nanofibers were measured with an image analysis software (JMicroVision V.1.2.7, Switzerland). The alignment of fibers was determined as the number of fibers oriented in a specified direction respecting to a perpendicular reference line (0° angles). The angles from which particular fibers diverged from this line were measured (n = 50) using the image analysis software. The data were expressed as a frequency in a histogram (Lee et al., 2005). The narrow distribution of nanofiber angles indicates a higher alignment.

#### 2.3.2. Mechanical characterizations

The tensile strength of nanofibers spun at different rotation speeds of the collector was evaluated using a texture analyzer with a 5-kg load cell appointed with grips holder (n = 5). For this purpose, the nanofiber mats with comparable weight per area were used. The size of each specimen was 6 × 35 mm in a rectangular shape. For all types of nanofibers, the stretch was applied in parallel and perpendicular direction.

#### 2.3.3. The physical state of alpha-arbutin

The X-ray diffraction pattern of alpha-arbutin, CA, and alpha-arbutin-loaded nanofibers spun at different rotation speeds of collector were analyzed using an X-ray powder diffractometer. Samples were exposed to monochromatized CuKα radiation after passing through Nickel filters and then were scrutinized between 5° and 50° (2theta). The voltage and current applied were 30 kV and 15 mA, respectively.

### 2.4. Alpha-arbutin content analysis

The alpha-arbutin-loaded nanofiber mats were cut (2 × 2 cm<sup>2</sup>) and weighed. The drug content in the CA nanofibers was quantified by exhaustive extraction of drug from the nanofibers by placing the nanofibers in 5 mL of deionized water and sonicated at 50 °C. After 1 h, the extraction medium was centrifuged, and the supernatant was collected. The extraction was repeated twice to ensure the complete extraction of the drug and all the supernatants were pooled. The drug content was then determined in triplicate using an HPLC connected to a C-18 column (150 × 4.60 mm, 5 μm). The injection volume was 100 μL. The samples were eluted with a mobile phase composed of (89:10:1) water:methanol:0.1 M hydrochloric acid flowing at 1.0 mL/min. UV detector set at 222 nm was used for the content analysis. The percentages of drug loading efficiency and loading capacity were computed by Eqs. (1) and (2), respectively:

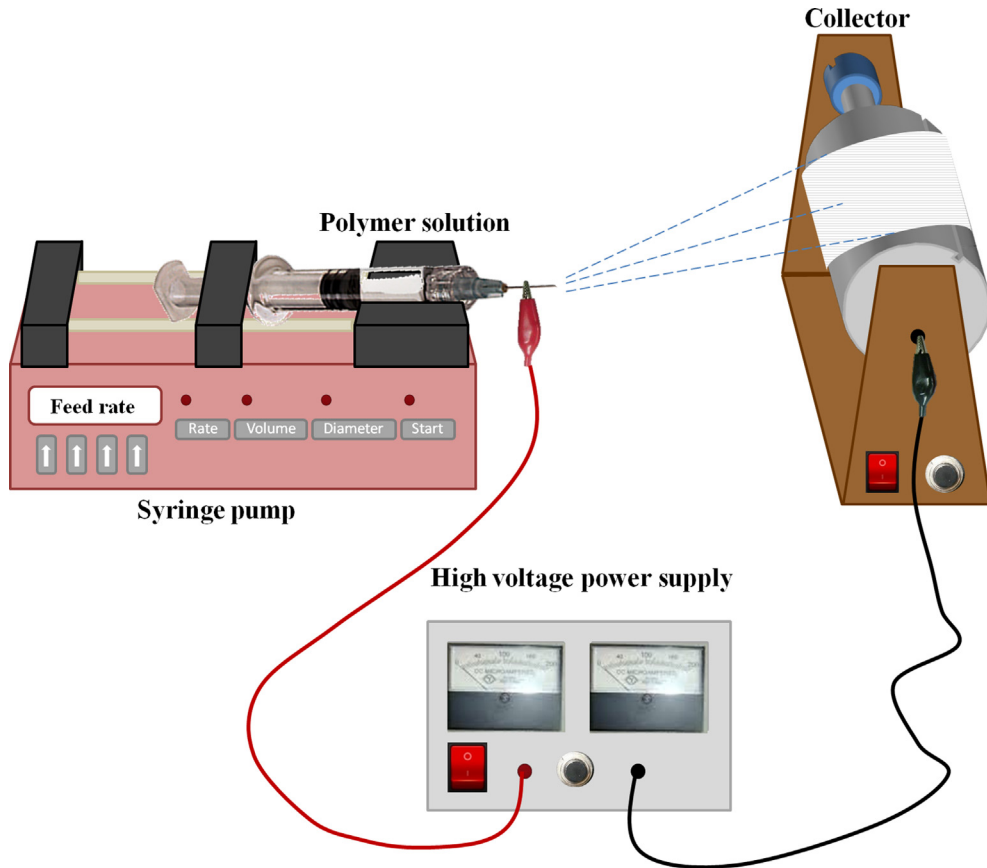


Fig. 1. Schematic representation of the electrospinning apparatus setup.

Loading efficiency (%)

$$= \frac{\text{Actual AR content } (\mu\text{g of AR/gm of nanofibers})}{\text{Theoretical AR content } (\mu\text{g of AR/gm of nanofibers})} \times 100 \quad (1)$$

$$\text{Loading capacity } (\%) = \frac{P_t}{M_t} \times 100 \quad (2)$$

where  $P_t$  is the amount of alpha-arbutin in the nanofiber mats, and  $M_t$  is the weight of nanofiber mats.

### 2.5. Drug release study

The release characteristics of alpha-arbutin from the alpha-arbutin-loaded nanofiber mats with different degree of fiber alignment were studied. The nanofibers were cut into the size of  $2 \times 2 \text{ cm}^2$ , removed from the backing foil, and then weighed. The nanofibers with a comparable weight per area were used for the comparison study of drug release. The nanofibers were submerged in 25 mL of deionized water contained in a glass bottle. The release experiment was performed at  $30 \pm 1 \text{ }^\circ\text{C}$  with constant shaking at 200 rpm. At a given time (0.25, 0.5, 0.75, 1, 3, 5, 10, 20, 30, 45 min), an aliquot of 500  $\mu\text{L}$  samples were withdrawn from the medium and replaced with an equal volume of fresh medium to maintain sink conditions. The drug content in the sample was quantified by HPLC.

### 2.6. Statistical analysis

All investigations were done in triplicate. The results are displayed as mean  $\pm$  standard deviation. The difference between the

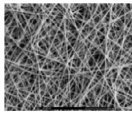
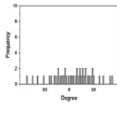
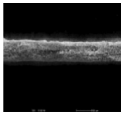
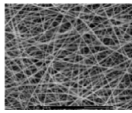
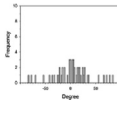
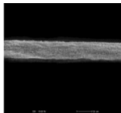
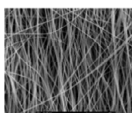
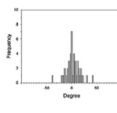
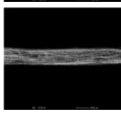
data was determined by a one-way analysis of variance (ANOVA) (Microsoft Excel). The significance level was set to  $p < 0.05$ .

## 3. Results and discussion

### 3.1. Characteristics of the alpha-arbutin-loaded nanofibers

Fiber arrangement can be altered by modifying the rotation speed of collector. (Yuan et al. 2017). In the present study, drum speeds were varied to obtain the fibers with different alignments. However, since high rotation speed could generate more air turbulence and wind which scattered the nanofibers during electrospinning and resulted in the lowered amount of fibers collected on the drum, the longer spin times were used for the fabrication of nanofibers with higher different degrees of alignment in which high rotation speeds were employed in order to obtain all types of the nanofiber mats with comparable weight per area. Table 1 presents the SEM images, alignment, diameters, and thickness of the alpha-arbutin-loaded nanofibers. Overall, smooth, uniform and bead-free nanofibers were obtained. Increasing the rotation speed of the drum collector from 350 to 2000 and 6000 rpm resulted in the nanofibers with a random, partially, and highly aligned orientation, respectively. This finding is in concordance with a previous study on cellulose nanofibers electrospun using a high speed rotating collector (300 m/min) (He et al., 2014). The diameters of the nanofibers ranged from 616 to 624 nm, which were not statistically different among the different types of the nanofibers. By using the different spin times as described earlier, the RA, PA, and HA nanofibers had a comparable weight per area of about  $0.0025 \text{ g/cm}^2$ . Nevertheless, their layer thickness was slightly different. In the case of HA nanofibers, which had the thinnest layers, it was

**Table 1**  
Effect of collector's rotation speed on fiber morphology, alignment, diameters, and layer thickness of AR-loaded nanofibers.

Nanofibers	Characteristics of nanofibers					
	Speed of collector (rpm)	SEM (Top view)	Alignment	Diameter (nm)	SEM (cross section)	Layer thickness ( $\mu\text{m}$ )
RA	350			$624 \pm 40$		$54 \pm 1$
PA	2000			$616 \pm 38$		$48 \pm 1$
HA	6000			$620 \pm 43$		$42 \pm 4$

possible that they were deposited tightly onto the collector and the inter-fiber arrangement was in a highly ordered manner as a result of a high stretching force generated by high-speed drum rotation.

### 3.2. Mechanical characteristics

The tensile strength of the differently aligned alpha-arbutin-loaded nanofibers were evaluated, and the results are presented in Table 2. It was found that different types of nanofibers possessed different tensile strength values depending on their alignments, as well as the direction of pulling force applied in the experiments. The HA nanofiber mats exhibited the lowest tensile strength and the applied force only separated the fibers apart without tearing when they were pulled in a perpendicular direction to the fiber alignment (Fig. 2). In contrast, when the mats were pulled in the direction parallel to the fiber alignment, the assembly of parallel nanofibers as bundles provided the robust resistance to the stretch. Consequently, this type of nanofibers showed the highest tensile strength value before the intra-fibrous breakage occurred. No difference of tensile strength was observed for the RA nanofibers even they were pulled in different directions. For the PA nanofibers, the mechanical behavior was in between those of the RA and HA nanofibers. This finding was in concordance with a previous study by He et al. (2014). However, Subramanian and coworkers fabricated 2D random and 3D longitudinally oriented nanofibers of poly(lactide-co-glycolide) (PLGA) by the adapted electrospinning method. The finding revealed that the tensile strength and Young's modulus of random PLGA fibers were significantly greater than those of the aligned PLGA nanofibers ( $p < 0.05$ ) (Subramanian et al., 2011). This difference might be contributed to the disregard of the direction of pulling force applied in their experiments.

### 3.3. The physical state of alpha-arbutin in nanofibers

Since the physical state of a drug may influence its solubility, XRD measurements were undertaken to reveal whether alpha-

arbutin in the nanofibers was present in the crystalline or amorphous state. The XRD patterns of the alpha-arbutin, CA, and the three types of alpha-arbutin-loaded nanofibers are presented in Fig. 3. The diffractogram of the alpha-arbutin shows sharp crystalline peaks, specifying its vast extent of crystallinity. However, no such peak was observed in the diffractograms of all types of the alpha-arbutin-loaded nanofibers, suggesting that alpha-arbutin was loaded into CA nanofibers in an amorphous form in all types of the nanofibers. However, it should be noted that the amorphous drug can recrystallized back to its crystalline state if the nanofibers are stored at high temperature and humidity. Nevertheless, the recrystallization is usually less favoured at normal storage condition at low temperature and humidity (Paaver et al., 2015). Therefore, the nanofibers should be stored in a water-impermeable packaging and stored at low temperature to prevent the recrystallization the drug in the nanofibers.

### 3.4. Drug loading efficiency in nanofibers

The content of alpha-arbutin in each nanofiber mats determined as the percentage loading efficacy and loading capacity are presented in Table 3. The actual amounts of alpha-arbutin incorporated in the nanofibers and loading efficiency were determined using an HPLC. In general, the amounts of alpha-arbutin in all types of samples were in the range of 2.7–2.8% w/w (weight of drug to weight of nanofibers). As calculated based on the theoretical content (3%w/w), the drug loading efficiencies were found to be more than 90% (Table 3), demonstrating that alpha-arbutin was successfully loaded into the nanofibers. In addition, the small standard deviation values implied that the drug was uniformly dispersed over different areas of the nanofiber mats. The discrepancy from the ideal value of 100% for the actual content could be due to the small amount of drug which was not extracted into the medium for HPLC assay and remained inside the fibers.

### 3.5. Drug release

The drug release from nanofibers was examined in water. The nanofiber mats with comparable weight and area were used to represent the nanofibers with the same quantities of the drug and polymer as well as the surface area. For all types of nanofibers, the release of alpha-arbutin was rapid, and the maximum cumulative amounts (84.0–86.1%) were achieved in 10 min (Fig. 4). It was hypothesized that the fast release happened via the rapid dissolution of the drug once water penetrated into the fiber layers, followed by the diffusion of the drug from the matrix through the

**Table 2**  
Tensile strength ( $\text{N}/\text{mm}^2$ ) of alpha-arbutin-loaded nanofiber mats ( $n = 5$ ). The stretching force was applied in the direction parallel or perpendicular to the fiber alignment direction.

Alignment of nanofibers	Tensile strength ( $\text{N}/\text{mm}^2$ )	
	Parallel stretching	Perpendicular stretching
Randomly aligned	$19.0 \pm 3.2$	$18.2 \pm 2.6$
Partially aligned	$70.1 \pm 9.5$	$14.4 \pm 3.7$
Highly aligned	$226.6 \pm 18.0$	$8.3 \pm 1.0$

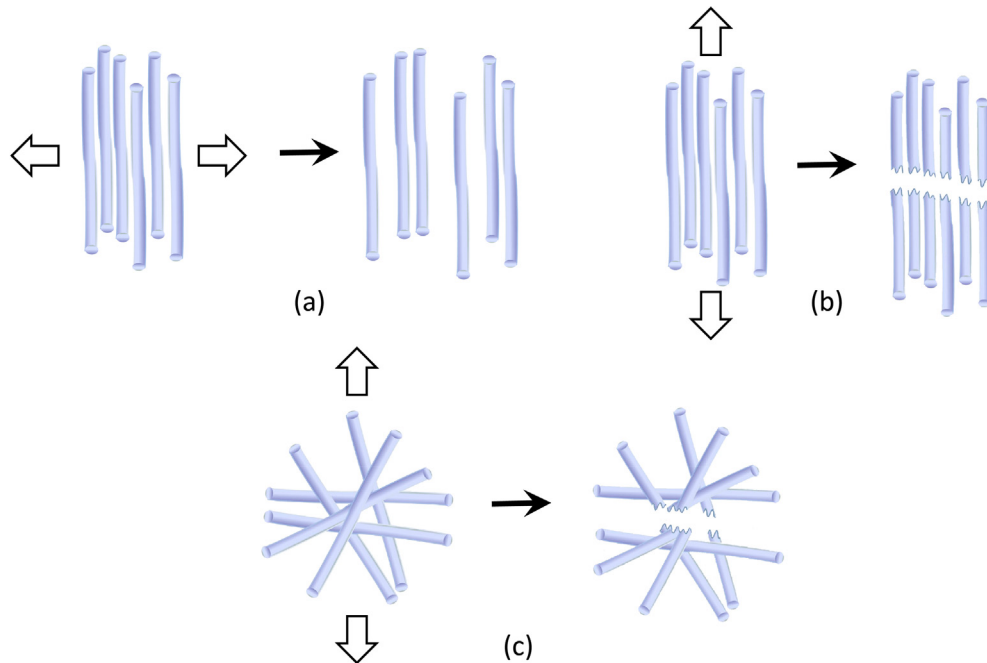


Fig. 2. Proposed illustrations of nanofibers with different alignments upon being stretched in parallel and perpendicular directions; (a) and (b) HA, (c) RA nanofibers.

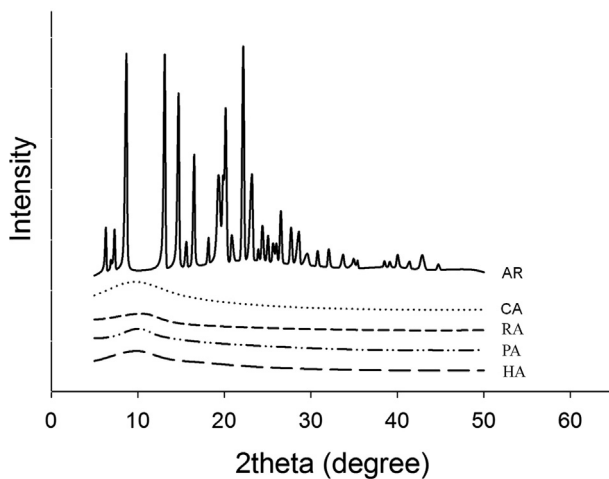


Fig. 3. Powder X-ray diffractograms of the AR, CA, and the three types of CA nanofibers.

Table 3

Loading efficiency and loading capacity of alpha-arbutin in the RA, PA and HA nanofibers (n = 3).

	RA	PA	HA
Loading efficiency (%)	91.6 ± 0.7	93.4 ± 0.8	95.9 ± 1.2
Loading capacity (%)	2.7 ± 1.1	2.7 ± 0.6	2.8 ± 1.4

water-filled channels in the entangled network of nanofibers into the medium. The dissolution and/or erosion of the CA nanofibers should not take part in the drug release since CA is water-insoluble polymer, and the nanofibers were found to erode at a minimal rate (data not shown). Interestingly, the fastest drug release was obtained from the HA nanofibers, followed by the PA and then the random ones, where 80% of drug was released in 1.7, 4.2, and 9.4 min, respectively (Fig. 4). From these results, it can be concluded that the drug release patterns during the initial

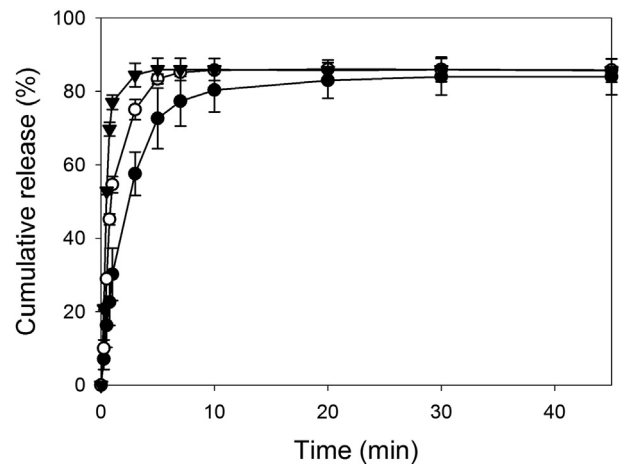


Fig. 4. Percent cumulative release of AR from nanofibers; (▼) HA, (○) PA, (●) RA nanofibers (n = 3).

burst period were significantly affected by the orientation of nanofibers. In the case of alpha-arbutin, the solubility of the drug should not be an influencing factor on the drug release since alpha-arbutin is freely soluble. In addition, it was all present in the amorphous form and contained at the comparable amounts in all types of nanofibers.

In the aspect of drug release, which is influenced by the fiber alignment, Meng et al. carried out their investigation using poly (lactide-co-glycolide) (PLGA), PLGA/gelatin, and PLGA/chitosan nanofibers loaded with poorly water-soluble fenbufen (Meng et al., 2011a, 2011b). They found that the release rate of the drug from the aligned nanofibrous scaffold to the aqueous medium was less than that from the randomly oriented nanofibers and they proposed that the aligned nanofibers had increased density and decreased pore size of scaffolds compared with the randomly oriented ones. Then, the apparent diffusion rate of the drug from the scaffold with aligned nanofibers was lower than that from the scaffold with random nanofibers. In addition, Eslamian et al

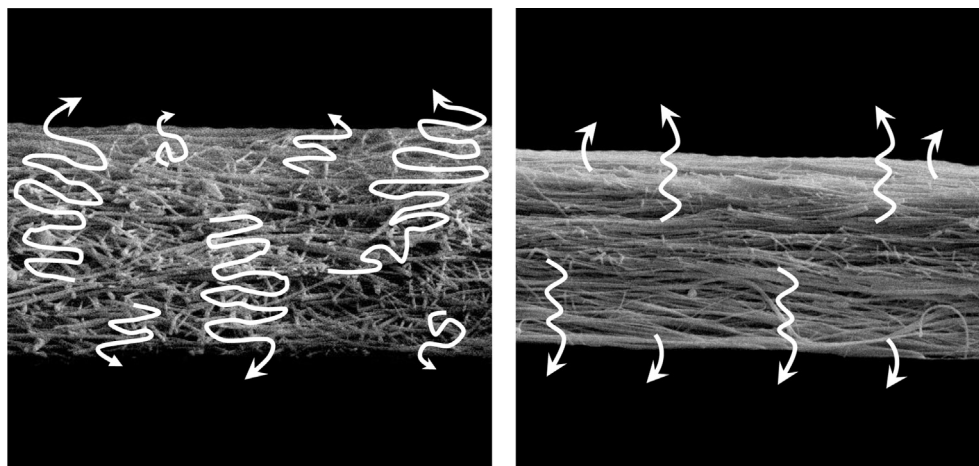


Fig. 5. Model of drug release from the HA (right) and RA (left) nanofibers.

also investigated the release of dexamethasone from randomly oriented and aligned hydrophobic PLGA nanofibers. They reported that the aligned fibers demonstrated less burst release and more sustained release compared to the random ones. They suggested that the slower release of the drug from the aligned fibers is presumably due to the presence of pores between fibers of the nanofibers that facilitate initial surface degradation of the randomly oriented fibers compared to the aligned fibers that are packed together (Eslamian et al., 2019). Conversely, in our study, the model compound is a hydrophilic drug which is different from the model hydrophobic drugs used in the studies by Meng et al and Eslamian et al. In addition, since PLGA is more hydrophobic and less water-permeable than CA, the proposed explanation by Meng et al and Eslamian et al may not be applied to our case. Moreover, in those works, the release profiles of fenbufen and dexamethasone were slow and sustained up to 25 h, whereas alpha-arbutin was rapidly released in 10 min in our experiments. The mechanisms of drug release should be therefore different between these two drugs from the different nanofibers.

In the present study, the alignment of nanofibers is assumed to be the key reason underlying the different rates of drug release. In the nanofibers with random alignment, a highly tangled network of fibers were formed. In case of the hydrophilic drug used in our study, the drug will have low affinity to remain in the nanofibers and will easily dissolve in water-filled inter-fibrous space after contact with water. Afterwards, the drug diffusing in the water-filled inter-fibrous space were retarded by lengthy and tortuous paths and thereby took a longer time to finally reach the external medium (Fig. 5). On the contrary, the HA nanofibers arranged in a more ordered fashion, and the entanglement was assumed to present at a lower degree. Therefore, the drug was able to move out to the external medium at a faster rate. This phenomenon is similar to the effect of Eddy diffusion in a chromatographic separation, where the solutes which travel along more tangled paths generated by the stationary phase particles spend longer time until they are eluted out of the column than those which move through the relatively straight shots (Kalinske and Pien, 1944).

From the results, it can be concluded that a faster drug release profile may be achieved by the control of nanofiber alignment. However, whether random or aligned scaffolds will give a faster rate probably depends on the properties of the drug and/or the polymer used. At least from our study, it was found that a prompt release of alpha-arbutin can be obtained from the fabrication of CA nanofibers in the highly-aligned orientation. This finding offers the

feasibility of using highly-aligned nanofibers in the delivery of certain drugs to obtain fast-releasing or fast-acting formulations.

#### 4. Conclusion

Various parameters, including the type of polymers, nanofiber diameter, porosity, geometry, and morphology has previously been reported to affect the release of a drug from nanofibers. In this study, these factors were controlled to study the effects of fiber alignment on the drug release. It was found that the fastest drug release was obtained from the HA nanofibers, followed by the PA and then the RA ones. The difference in the release profiles may be due to the diffusion paths of the drug from the nanofibers, in which the HA nanofibers were assumed to have the shortest path length. However, this effect depends on the type of drugs and polymers used. In the case of hydrophobic polymers containing a hydrophilic drug, faster drug release could be obtained with a higher degree of fiber alignment.

#### Declaration of Competing Interest

The authors declare that they have no known competing financial interests or personal relationships that could have appeared to influence the work reported in this paper.

#### Acknowledgment

We would like to express gratitude to the Faculty of Pharmacy, Silpakorn University, for the facility support. This research did not receive any specific grant from funding agencies in the public, commercial, or not-for-profit sectors.

#### References

- Akhgari, A., Shakib, Z., Sanati, S., 2017. A review on electrospun nanofibers for oral drug delivery. *Nanomed. J.* 4, 197–207. <https://doi.org/10.22038/NMJ.2017.04.001>.
- Chou, S.F., Woodrow, K.A., 2017. Relationships between mechanical properties and drug release from electrospun fibers of PCL and PLGA blends. *J. Mech. Behav. Biomed. Mater.* 65, 724–733. <https://doi.org/10.1016/j.jmbbm.2016.09.004>.
- Eslamian, M., Khorrami, M., Yi, N., Majid, S., Abidian, M.R., 2019. Electrospinning of highly aligned fibers for drug delivery applications. *J. Mater. Chem. B* 7, 224–232. <https://doi.org/10.1039/c8tb01258j>.
- Fathi-Azarbayjani, A., Qun, L., Chan, Y.W., 2010. Novel vitamin and gold-loaded nanofiber facial mask for topical delivery. *AAPS PharmSciTech.* 11, 1164–1170. <https://doi.org/10.1208/s12249-010-9475-z>.
- Haider, A., Haider, S., Kang, I.-K., 2018. A comprehensive review summarizing the effect of electrospinning parameters and potential applications of nanofibers in

- biomedical and biotechnology. *Arab. J. Chem.* 11, 1165–1188. <https://doi.org/10.1016/j.arabjc.2015.11.015>.
- He, X., Xiao, Q., Lu, C., Wang, Y., Zhang, X., Zhao, J., Zhang, W., Zhang, X., Deng, Y., 2014. Uniaxially aligned electrospun all-cellulose nanocomposite nanofibers reinforced with cellulose nanocrystals: scaffold for tissue engineering. *Biomacromolecules* 15, 618–627. <https://doi.org/10.1021/bm401656a>.
- Hu, X., Liu, S., Zhou, G., Huang, Y., Xie, Z., Jing, X., 2014. Electrospinning of polymeric nanofibers for drug delivery applications. *J. Control. Release* 185, 12–21. <https://doi.org/10.1016/j.jconrel.2014.04.018>.
- Kalinske, A.A., Pien, C.L., 1944. Eddy diffusion. *Ind. Eng. Chem.* 36, 220–223. <https://doi.org/10.1021/ie50411a008>.
- Khoshevisan, K., Maleki, H., Samadian, H., Shahsavari, S., Sarrafzadeh, M.H., Larijani, B., Dorkoosh, F.A., Haghpanah, V., Khorramizadeh, M.R., 2018. Cellulose acetate electrospun nanofibers for drug delivery systems: Applications and recent advances. *Carbohydr. Polym.* 198, 131–141. <https://doi.org/10.1016/j.carbpol.2018.06.072>.
- Konwarh, R., Karak, N., Misra, M., 2013. Electrospun cellulose acetate nanofibers: The present status and gamut of biotechnological applications. *Biotechnol. Adv.* 31 (4), 421–437. <https://doi.org/10.1016/j.biotechadv.2013.01.002>.
- Lee, C.H., Shin, H.J., Cho, I.H., Kang, Y.M., Kim, I.A., Park, K.D., Shin, J.W., 2005. Nanofiber alignment and direction of mechanical strain affect the ECM production of human ACL fibroblast. *Biomaterials* 26, 1261–1270. <https://doi.org/10.1016/j.biomaterials.2004.04.037>.
- Maeda, K., Fukuda, M., 1996. Arbutin: Mechanism of its depigmenting action in human melanocyte culture. *J. Pharmacol. Exp. Ther.* 276, 765–769.
- Meng, Z.X., Xu, X.X., Zheng, W., Zhou, H.M., Li, L., Zheng, Y.F., Lou, X., 2011a. Preparation and characterization of electrospun PLGA/gelatin nanofibers as a potential drug delivery system. *Colloids. Surf. B. Biointerfaces* 84, 97–102. <https://doi.org/10.1016/j.colsurfb.2010.12.022>.
- Meng, Z.X., Zheng, W., Li, L., Zheng, Y.F., 2011b. Fabrication, characterization and in vitro drug release behavior of electrospun PLGA/chitosan nanofibrous scaffold. *Mater. Chem. Phys.* 125, 606–611. <https://doi.org/10.1016/j.matchemphys.2010.10.010>.
- Paaver, U., Heinämäki, J., Laidmäe, I., Lust, A., Kozlova, J., Sillaste, E., Kirsimäe, K., Veski, P., Kogermann, K., 2015. Electrospun nanofibers as a potential controlled-release solid dispersion system for poorly water-soluble drugs. *Int. J. Pharm.* 479, 252–260. <https://doi.org/10.1016/j.ijpharm.2014.12.024>.
- Perissutti, B., Rubessa, F., Moneghini, M., Voinovich, D., 2003. Formulation design of carbamazepine fast-release tablets prepared by melt granulation technique. *Int. J. Pharm.* 256, 53–63. [https://doi.org/10.1016/s0378-5173\(03\)00062-0](https://doi.org/10.1016/s0378-5173(03)00062-0).
- Pillay, V., Dott, C., Choonara, Y., Tyagi, C., Tomar, L., Kumar, P., du Toit, L.C., Ndesendo, V.M.K., 2013. A review of the effect of processing variables on the fabrication of electrospun nanofibers for drug delivery applications. *J. Nanomater.* <https://doi.org/10.1155/2013/789289>.
- Sarkar, R., Arora, P., Garg, K.V., 2013. Cosmeceuticals for Hyperpigmentation: What is Available?. *J. Cutan. Aesthet. Surg.* 6 (1), 4–11. <https://doi.org/10.4103/0974-2077.110089>.
- Subramanian, A., Krishnan, U.M., Sethuraman, S., 2011. Fabrication of uniaxially aligned 3D electrospun scaffolds for neural regeneration. *Biomed. Mater.* 6. <https://doi.org/10.1088/1748-6041/6/2/025004> 025004.
- Teo, W.E., Ramakrishna, S., 2006. A review on electrospinning design and nanofibre assemblies. *Nanotechnology* 17, R89–R106. <https://doi.org/10.1088/0957-4484/17/14/R01>.
- Thenmozhi, S., Dharmaraj, N., Kadirvelu, K., Kim, H.Y., 2017. Electrospun nanofibers: new generation materials for advanced applications. *Mater. Sci. Eng. B* 217, 36–48. <https://doi.org/10.1016/j.mseb.2017.01.001>.
- Tonglairoom, P., Ngawhirunpat, T., Rojanarata, T., Kaomongkolgit, R., Opanasopit, P., 2014. Fast-acting clotrimazole composited PVP/HPbetaCD nanofibers for oral candidiasis application. *Pharm. Res.* 31, 1893–1906. <https://doi.org/10.1007/s11095-013-1291-1>.
- Tonglairoom, P., Ngawhirunpat, T., Rojanarata, T., Kaomongkolgit, R., Opanasopit, P., 2015. Fabrication of a novel scaffold of clotrimazole-microemulsion-containing nanofibers using an electrospinning process for oral candidiasis applications. *Colloids Surf B Biointerfaces* 126, 18–25. <https://doi.org/10.1016/j.colsurfb.2014.12.009>.
- Vong, M., Radacsi, N., 2018. Fabrication of radially aligned electrospun nanofibers in a three-dimensional conical shape. *Electrospinning* 2, 1–14. <https://doi.org/10.1515/esp-2018-0001>.
- Yuan, H., Zhou, Q., Zhang, Y., 2017. Improving fiber alignment during electrospinning. In: Afshari, M. (Ed.), *Electrospun Nanofibers*. Woodhead Publishing, Cambridge, pp. 125–147.